Activity of Homogeneous Chromium(III)-Based Alkene Polymerization Catalysts: Lack of Importance of the Barrier to Ethylene Insertion

Vidar R. Jensen,* Klaus Angermund, and Peter W. Jolly

Max-Planck Institut für Kohlenforschung, D-45470 Mülheim an der Ruhr, Germany

Knut J. Børve

Department of Chemistry, University of Bergen, N-5007 Bergen, Norway

Received August 17, 1999

The barrier to ethylene insertion into the chromium−methyl bond in $Cp(H_2O)CrMe^+$ (**1**), $Cp(THF)CrMe^+$ (**2**), Cp(imidazol-2-ylidene)$CrMe^+$ (**3**), $(H_2NC_2H_4C_5H_4)CrMe^+$ (**4**), and $(Me_2NC_2H_4C_5H_4)CrMe^+$ (**5**) has been calculated using gradient-corrected density functional theory (DFT) and compared to experimentally recorded activity data for homogeneous Cr(III)-based polymerization catalysts. The lack of correlation between the two data sets shows that the observed differences in activity among these catalysts do not originate from a difference in the ability of the various $Cp(donor)CrR^+$ complexes to instigate the bond-breaking and -forming phases of the Cossée−Arlman-type insertion step. Rather, the superior performance of the donor-substituted Cp−Cr catalysts is probably associated with the enforced proximity of the donor group to the metal, demonstrating the importance of the constant presence of the donor ligand in the inner coordination sphere of the chromium atom. For **5**, insertion of a second ethylene molecule has also been investigated, and the results reflect that for the Cr(III)-based catalysts the insertion step does not represent a serious bottleneck in the propagation cycle, consistent with the observed high activities of the recently developed amino-substituted Cp−Cr catalysts.

1. Introduction

The fact that two of the commercially most important catalysts for the polymerization of ethylene, the Phillips[1,2] and Union Carbide[3,4] silica-supported catalysts, are based on chromium has inspired efforts to prepare homogeneous counterparts. This task has proved difficult and, although some progress has been made in recent years, reports of homogeneous chromium-based polymerization catalysts are scarce compared to those of group 4 based catalysts. These results have already been reviewed,[5,6] and here we restrict ourselves to noting that, among the low-valent states of chromium, oxidation state +III stands out as the most active for the polymerization of ethylene. The contemporary Cr(III)-based catalysts are typically donor-stabilized alkyls or halides with a (substituted) cyclopentadienyl group as one of the ligands. With the donor (e.g., amino group) bridged to the Cp and with methylalumoxane (MAO) as cocatalyst, Jolly et al.[7−9] have obtained activities of 1×10^4 kg of PE/((mol of Cr) h) at 2 bar and room temperature. Closely related systems such as $[CrCp^*(THF)_2Me]^+BPh_4^-$ [10,11] display activities orders of magnitude lower, although in both cases it is assumed that a three-coordinate cation of the general type $Cp(donor)CrR^+$ (where Cp is a (substituted) cyclopentadienyl ligand) constitutes the active species. Recent variations of the donor ligand in (substituted) cyclopentadienylchromium(III) complexes also include carbenes in the form of 1,3-disubstituted imidazol-2-ylidenes.[9,12] However, as described in the preceding article,[9] the activity for the polymerization of ethylene shown by the Cp(tetramethylimidazol-2-ylidene)$CrCl_2$ catalyst is disappointing, and in this respect the carbene catalyst seems to resemble the Cr−tetrahydrofuran complexes[10,11] rather than the amino-substituted Cp systems.

The dramatic differences in activity for ethylene polymerization for these chemically closely related systems call for further investigation. One possible explanation for the differences is simply that, although the catalysts are indeed related, the structural variations are sufficiently pronounced to significantly influence the barrier to ethylene insertion. A quantum-

(1) Hogan, J. P.; Banks, R. L. (Phillips Petroleum Co.) Belg. Patent 530,617, 1955; U.S. Patent 2825,721, 1958.
(2) Hogan, J. P. *J. Polym. Sci. A* **1970**, *8*, 2637.
(3) Karapinka, G. L., U.S. Patent 3,709,853, 1973.
(4) Karol, F. J.; Karapinka, G. L.; Wu, C.; Dow, A. W.; Johnson, R. N.; Garrick, W. L. *J. Polym. Sci. A* **1972**, *10*, 2621.
(5) Theopold, K. H. *CHEMTECH* **1997**, *27*, 26−32.
(6) Theopold, K. H. *Eur. J. Inorg. Chem.* **1998**, 15.
(7) Emrich, R.; Heinemann, O.; Jolly, P. W.; Krüger, C.; Verhovnik, G. P. J. *Organometallics* **1997**, *16*, 1511.
(8) Jolly, P. W.; Jonas, K.; Verhovnik, G. P. J.; Döhring, A.; Göhre, J.; Weber, J. C. (Studiengesellschaft Kohle mbH) WO-A 98/04570, 1998.
(9) Döhring, A.; Göhre, J.; Jolly, P. W.; Kryger, B.; Rust, J.; Verhovnik, G. P. J. *Organometallics* **2000**, *19*, 388.
(10) Thomas, B. J.; Theopold, K. H. *J. Am. Chem. Soc.* **1988**, *110*, 5902.
(11) Thomas, B. J.; Noh, S. K.; Schulte, G. K.; Sendlinger, S. C.; Theopold, K. H. *J. Am. Chem. Soc.* **1991**, *113*, 893.
(12) Voges, M. H.; Rømming, C.; Tilset, M. *Organometallics* **1999**, *18*, 529.

10.1021/om9906666 CCC: $19.00
Publication on Web 01/21/2000

Chart 1

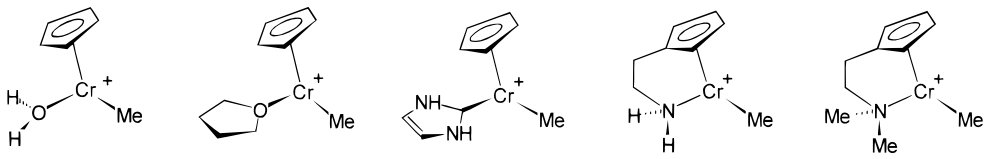

1 **2** **3** **4** **5**

chemical study[13] of $Cl(H_2O)CrMe^+$ as a model for such three-coordinate cations of chromium(III) has already demonstrated that the latter has a low (~8 kcal/mol) barrier for ethylene insertion.[14−16] Here, we extend this study to a series of Cr(III)-based complexes and include realistic models of several recently developed catalysts.

Catalysts based on group 4 metals with the oxidation state +IV (d^0) have been shown to insert alkenes with very low barriers, and it has been questioned whether the insertion step is actually rate-determining in these cases.[17] Catalysts based on metals with significant d population, however, may be expected to display more pronounced barriers to insertion,[13,18] and it is thus more likely that in these cases this reaction step determines the actual activity. We report here the use of gradient-corrected density functional theory (DFT) to compare the barrier to ethylene insertion with the observed catalytic activity by studying the initial insertion step into the Cr−Me bond for $Cp(H_2O)CrMe^+$ (**1**), Cp(THF)-$CrMe^+$ (**2**), Cp(imidazol-2-ylidene)$CrMe^+$ (**3**), $(H_2NC_2H_4C_5H_4)CrMe^+$ (**4**), and $(Me_2NC_2H_4C_5H_4)CrMe^+$ (**5**), as well as the second insertion step for **5** (see Chart 1).

2. Computational Details

This study was carried out using gradient-corrected density functional theory (DFT) with the gradient corrections included self-consistently during both geometry optimization and energy evaluation. Throughout this work we have employed the local exchange-correlation potential developed by Vosko et al.[19] augmented with Becke's[20] nonlocal exchange corrections along with Perdew and Wang's[21] nonlocal correlation corrections. All calculations were performed in the spin-unrestricted formulation, and at various points, tests were conducted to ensure that stable solutions had been obtained. For practical reasons, Figure 1 displays restricted open-shell orbitals, which for the systems in question are very similar to their unrestricted counterparts. Extensive studies reported elsewhere[13,22] show that the BPW91 functional is capable of providing accurate energy profiles for the monomer insertion step during metal-catalyzed olefin polymerization. Two different implementations of this functional were employed in the current work, and these are described below.

2.1. G94 Approach. For the complexes **1**−**4** we used the DFT facility as implemented in the Gaussian 94 set of programs,[23] and the results obtained are labeled G94 in the current work. Stationary points of ethylene insertion were optimized and characterized using algorithms involving analytic calculations of the first and second derivatives of the energy, respectively. Geometries were converged to a maximum force and displacement of 0.000 45 hartree/Bohr and 0.0018 Bohr, respectively. Thermochemical quantities were computed within the harmonic oscillator, rigid-rotor, and ideal-gas approximations. The basis sets employed were spherical-harmonics atom-centered Gaussian bases (denoted by basis B in ref 13) which consist of a triply split d shell on chromium, are of valence double-ζ plus polarization quality for first-row atoms, and employ a doubly split 1s for hydrogen. With the exception of the donating carbon atom of the carbene ligand in **3**, polarization functions were generally omitted for carbon atoms not forming part of the ethylene or the polymer chain. It has been specifically shown in ref 13 that augmenting these sets with one contracted f function on chromium and one uncontracted p function on each hydrogen belonging to the growing alkyl chain or the monomer has very little influence on the calculated relative energies of ethylene insertion.

2.2. ADF Approach. For complexes **4** and **5** we employed the Amsterdam Density Functional[24−26] package, and the results are labeled ADF in the current work. Geometries were converged to a maximum force of 0.001 hartree/Å or hartree/radian. The potential energy surface (PES) of ethylene insertion was investigated in a linear transit fashion where all degrees of freedom, except for the reaction coordinate (taken to be the carbon−carbon bond formed during insertion), were optimized in each step. For **5**, the C−H bond lengths of the methyl groups on nitrogen were constrained to be equal, which is expected to have a negligible effect on the shape of the calculated PES. The corresponding gradient elements still remain very low (absolute values ≤0.007 hartree/Å) and almost constant during the reaction. The transition states were obtained as the maximum on the potential energy curve of ethylene insertion. The difference between the resulting structure and the fully optimized, true transition state of ethylene insertion for a d^0 metal is reported to be minimal.[18] The ADF calculations were performed in parallel.[27] Slater-type bases from the ADF internal database[28,29] were used throughout, together with the frozen-core approximation. For chromium (valence: 3s, 3p, 3d, 4s, 4p), an uncontracted triple-ζ basis was applied. Carbon (valence: 2s, 2p) was described by a double-ζ basis, while for ethylenic C atoms as well as those in the growing polymer chain this set was augmented with a single 3d polarization function. For hydrogen (valence: 1s), a double-ζ basis was applied and augmented with a single 2p

(13) Jensen, V. R.; Børve, K. J. *Organometallics* **1997**, *16*, 2514.
(14) Cossée, P. *J. Catal.* **1964**, *3*, 80.
(15) Arlman, E. J. *J. Catal.* **1964**, *3*, 89.
(16) Arlman, E. J.; Cossée, P. *J. Catal.* **1964**, *3*, 99.
(17) Lohrenz, J. C. W.; Woo, T. K.; Ziegler, T. *J. Am. Chem. Soc.* **1995**, *117*, 12793.
(18) Margl, P.; Deng, L. Q.; Ziegler, T. *J. Am. Chem. Soc.* **1998**, *120*, 5517.
(19) Vosko, S. H.; Wilk, L.; Nusair, M. *Can. J. Phys.* **1980**, *58*, 1200.
(20) Becke, A. D. *Phys. Rev. A* **1988**, *38*, 3098.
(21) Perdew, J. P.; Wang, Y. *Phys. Rev. B* **1992**, *45*, 13244.
(22) Jensen, V. R.; Børve, K. J. *J. Comput. Chem.* **1998**, *19*, 947.
(23) Frisch, M. J.; Trucks, G. W.; Schlegel, H. B.; Gill, P. M. W.; Johnson, B. G.; Robb, M. A.; Cheeseman, J. R.; Keith, T.; Petersson, G. A.; Montgomery, J. A.; Raghavachari, K.; Al-Laham, M. A.; Zakrzewski, V. G.; Ortiz, J. V.; Foresman, J. B.; Peng, C. Y.; Ayala, P. Y.; Chen, W.; Wong, M. W.; Andres, J. L.; Replogle, E. S.; Gomperts, R.; Martin, R. L.; Fox, D. J.; Binkley, J. S.; Defrees, D. J.; Baker, J.; Stewart, J. P.; Head-Gordon, M.; Gonzalez, C.; Pople, J. A. Gaussian, Inc., Pittsburgh, PA, 1995.
(24) ADF 2.3.0; Theoretical Chemistry, Vrije Universiteit, Amsterdam, The Netherlands, 1997.
(25) Baerends, E. J.; Ellis, D. E.; Ros, P. *Chem. Phys.* **1973**, *2*, 41.
(26) te Velde, G.; Baerends, E. J. *J. Comput. Phys.* **1992**, *99*, 84.
(27) Fonseca Guerra, C.; Visser, O.; Snijders, J. G.; te Velde, G.; Baerends, E. J. In *Parallelisation of the Amsterdam Density Functional Program*; Clementi, E., Corongiu, G., Eds.; STEF: Cagliari, Italy, 1995; p 303.
(28) Vernoijs, P.; Snijders, J. G.; Baerends, E. J. *Slater-type Basis Functions for the Whole Periodic System*; Department of Theoretical Chemistry, Free University: Amsterdam, The Netherlands, 1981.
(29) Snijders, J. G.; Baerends, E. J.; Vernoijs, P. *At. Nucl. Data Tables* **1982**, *26*, 483.

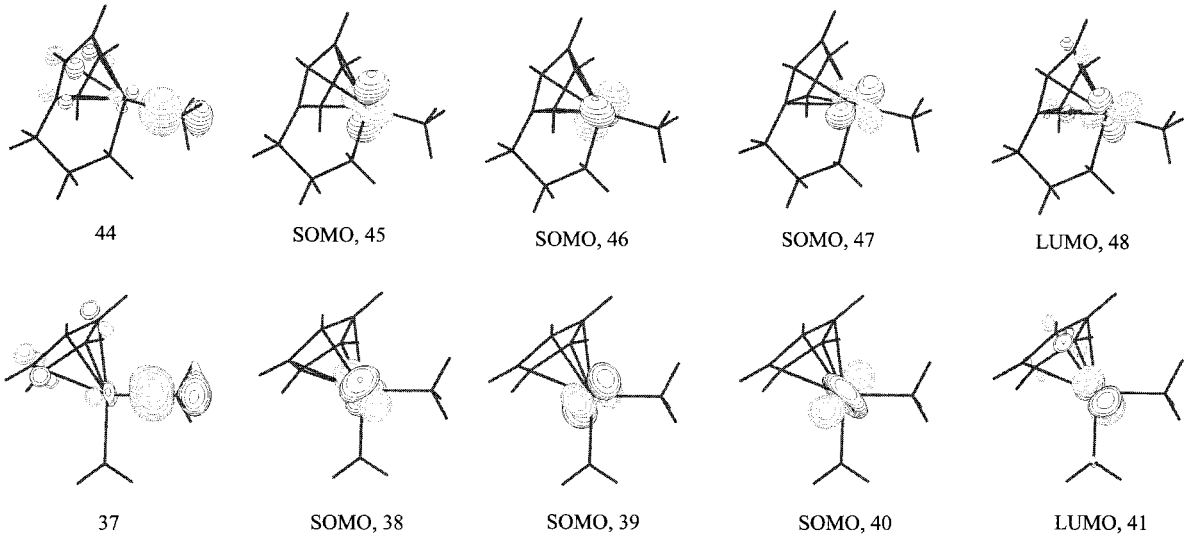

Figure 1. Frontier orbitals of $(H_2NC_2H_4C_5H_4)CrMe^+$ (**4**, upper row) and $Cp(H_2O)CrMe^+$ (**1**, lower row). The orbitals are depicted as isosurfaces at a value of 0.09 au using the MOLDEN[45] program. They were obtained within the restricted open-shell formulation (ROBPW91) with the structures optimized using the G94 approach as described in Computational Details.

polarization function for atoms belonging to ethylene as well as the growing polymer chain. A set of auxiliary[30] s, p, d, f, and g Slater functions centered on all nuclei was used in order to fit the molecular density and present Coloumb and exchange potentials accurately in each SCF cycle.

3. Results and Discussion

An important goal of the present work was to correlate the ease with which ethylene is inserted (as measured by the barrier calculated relative to the π complex) with the structure and properties of each catalyst. The complexes **1**−**5** differ mainly in the nature of the donor ligand, which varies from water, through tetrahydrofuran and amino groups, to a carbene. Thus, one may expect some variation among the metal−donor bonds, possibly accompanied by significant differences in the electronic structure of the catalysts. Therefore, the first subsection below is concerned with the metal−donor bond strengths and the influence of the donor on the frontier orbitals and electronic structure of the catalyst complex. Ethylene insertion is considered in the two following subsections.

3.1. Properties of the Catalyst Cation. 3.1.1. $CpCrMe^+$−Donor Bond Energies. To bypass the problem of comparing metal−donor bond strengths in bridged complexes such as **4** and **5** with those in complexes where the donors are not bridged to a covalent ligand, we decided to focus the investigation of metal−donor bond strengths on complexes of the type $CpCrMe^+$−donor. Instead of the two bridged-donor complexes, we used $Cp(NH_3)CrMe^+$ and $Cp(NMe_3)$-$CrMe^+$, and the metal−donor bond energies are given in Table 1 together with those of complexes **1**−**3**.

Considerable variance is seen among the bond energies in Table 1. The carbene ligand is found to be a very good donor, in accord with experimental findings,[31,32] and the complexation energy is almost twice that of the poorest donor, water. If electronic effects induced by the donor ligand are of any importance for the ethylene insertion reaction, the vast span in metal−donor bond strengths should guarantee that such electronic effects are indeed covered by the current study. Intermediate bond energies are found for THF, NH_3, and NMe_3, with less than 3 kcal/mol difference between ammonia and trimethylamine. The small difference in the latter case shows that NH_3 can be used as a model for larger, substituted amines—at least when one focuses on electronic effects. As a result, in the present study we should expect similar results for catalysts **4** and **5** and differences can mainly be attributed to the larger steric requirement of **5**. It is also gratifying that the agreement between the two computational approaches (G94 and ADF) is excellent, as evident from entries in Table 1, where both approaches have been applied to the same systems. Finally, the free energies of donor complexation (ΔG_{298}) are seen to be 12−14 kcal/mol less in favor of the adducts than the pure electronic energies, a difference that is mainly due to the reduction in entropy upon complexation of the donor. The zero-point vibrational contribution to this reduction in stability of the adducts is only 2−3 kcal/mol.

Table 1. $CpCrMe^+$−Donor Bond Dissociation Energies (kcal/mol)

donor	ΔE_e	ΔG_{298}
H_2O	36.1[a]	24.7[a]
THF	43.4,[a] 43.2[b]	29.3[a]
NH_3	45.2,[a] 44.7[b]	33.0[a]
NMe_3	47.4[b]	
imidazol-2-ylidene	66.2[b]	

[a] G94. [b] ADF.

Another important aspect of the catalyst−donor bond strengths is how they compare with those of cocatalyst−donor bonds. Accurate values for the latter are difficult to obtain, since the detailed structure and role of methylalumoxane (MAO) during the catalysis is not known. For simplicity, we assume that the strongest Lewis acid in, and thus the active species of, MAO is

(30) Krijn, J.; Baerends, E. J. *Fit Functions in the HFS Method*; Department of Theoretical Chemistry, Free University: Amsterdam, The Netherlands, 1984.
(31) Arduengo, A. J.; Harlow, R. L.; Kline, M. J. *J. Am. Chem. Soc.* **1991**, *113*, 361.
(32) Herrmann, W. A.; Köcher, C. *Angew. Chem.* **1997**, *109*, 2256.

actually trimethylaluminum (see comments in ref 9). The Me_3Al−water and Me_3Al−ammonia electronic bond dissociation energies are found to be 15.5 and 22.1 kcal/mol (using G94), whereas the corresponding bond energies for THF and imidazol-2-ylidene are 15.8 and 30.4 kcal/mol, respectively, as calculated using the ADF approach. These bonds are less than half as strong as the corresponding chromium−donor bonds listed in Table 1, indicating that (at least in the limit of complete charge separation and exclusion of solvent effects) the donor prefers to remain coordinated to the catalyst. Excess trimethylaluminum is thus needed before abstraction of the Lewis base occurs. It seems likely that the presence of solvent as well as the high cocatalyst/catalyst ratios of Ziegler catalysts may result in abstraction of the donor despite relatively large catalyst−donor bond energies. If we assume that presence of the donor ligand is important for obtaining catalytic activity, correlation between the catalyst−donor bond strength (or alternatively the difference between the donor bond strength of the catalyst and cocatalyst) and the observed catalytic activity should be expected. The carbene ligand has by far the largest catalyst−donor bond energy and also the largest difference in donor bond energy between catalyst and cocatalyst (35.9 kcal/mol). The carbene complex should thus have a higher catalytic activity than other nonbridged donors, in accord with experiment.[33] However, even if a better model of the acidic centers of MAO could be obtained, a more accurate investigation of the relative stability of the catalyst−donor complexes will require modeling of the catalyst−cocatalyst contact as well as solvent effects.

3.1.2. Frontier-Orbital Picture of the Catalyst Cation. For the reactant complexes $(H_2NC_2H_4C_5H_4)$-$CrMe^+$ (**4**) and $Cp(H_2O)CrMe^+$ (**1**), the orbitals of main interest are included in the upper and lower rows of Figure 1, respectively. As far as polymerization is concerned, the properties of the metal−alkyl bond and the low-energy virtual orbitals at the metal are of interest. The highest lying orbitals with Cr−C bond character (no. 44 and 37 for **4** and **1**, respectively) are similar and show good directionality and a shape consistent with a d_σ−p_σ bond. The Cr−C bond originates mainly from a $3d_{z^2}$-rich lowest unoccupied orbital (LUMO) in the C_{2v}-like fragment Cp(donor)Cr^+. For d^0 metal-based catalysts, this d_{z^2}-dominated orbital is often found to be of rather high energy,[34,35] and the bond to the alkyl group is thus formed through hybridization with the d_{xz} and $d_{x^2-y^2}$ orbitals and is associated with deformation toward a pyramidal structure. For complexes based on Cr(III), the higher d-occupation reduces the energy gap to the d_{z^2} orbital and is accompanied by an increase in stability for the planar arrangement in the three-coordinate Cr−alkyl cations. For **4**, the energetic preference for a pyramidal compared to a trigonal-planar arrangement (the transition state of inversion) is only 1.1 kcal/mol, whereas for **1** as well as the other complexes with unbridged (free) donor ligands, the trigonal-planar arrangement is preferred. For d^0 metal-based catalysts, the barrier to planarity has been found to correlate with the barrier to monomer insertion,[18,35] and thus, solely on the basis of the high stability of the planar configuration, rather low barriers to ethylene insertion should be expected for the catalysts **1**−**5**. In addition, only minor differences exist between the three singly occupied (SOMO's) and the LUMO orbitals for **1** and **4**. The frontier orbitals for the carbene complex **3** also resemble those pictured in Figure 1. To summarize, the frontier orbitals of **1**−**5** are qualitatively similar despite the marked difference in metal−donor bond strength.

One might also expect that the presence of dative ligands with very different donor abilities should influence a simple, scalar property such as the charge on the metal. However, this does not seem to be the case for **1**, **3**, and **4** (Mulliken charges on Cr are 0.74, 0.70, and 0.69 e, respectively). Again, the conclusion is that, although the dative ligands chosen for the study are indeed different, this has little effect on the electronic structure for the three-coordinate, cationic methyl complexes and one might therefore expect similar catalytic performance.

3.2. Initial Ethylene Insertion Step. In this section, detailed analyses of energetic, geometric, and electronic aspects of the initial ethylene insertion step for the complexes **1**−**5** are presented. Insertion of a second ethylene molecule is discussed for complex **5** in the next section.

3.2.1. Geometric Structures. The geometrical features of the stationary points along the reaction path of ethylene insertion are found to be very similar for the current model catalysts, and we thus limit the graphical representation to complex **5** (Figure 2). The most important geometrical parameters for the reactants, the metal−ethylene complexes, and the transition states for all complexes studied are given in Table 2. It is apparent that these stationary points resemble those expected for the Cossée−Arlman mechanism, which are well-known from theoretical investigations of d^0 metal-based catalysts (for example, see refs 18, 34, 36, and 37). The similarity to structures obtained in our study[13] of the small model system $Cl(H_2O)CrMe^+$ is also evident. The three-coordinate reactant complexes with bridged donors (**4** and **5**) are weakly bent (pyramidal), as judged from $\theta_p \approx 10°$, the deviation from 360° of the sum of the three primary bond angles around chromium. The complexes with nonbridged (or free) donors, on the other hand, are planar with θ_p being zero or close to zero. The position of the donor relative to chromium is to a large extent determined by the relatively short ethano bridge in **4** and **5**, the Cp−Cr−(donor) angles being ∼25° more acute than in the complexes with free donors. A weak α-agostic interaction involving a lengthening of the C−H bond of 1−2 pm is observed in all reactant complexes. Coordination of ethylene causes deformation of the planar or close to planar three-coordinate fragment, and the π complexes may all be characterized as having distorted-tetrahedral structures with the θ_p value being

(33) Following a reviewer's suggestion, we have compared the activities for ethylene polymerization of $Cp(THF)CrCl_2$/MAO and Cp-(tetramethylimidazol-2-ylidene)$CrCl_2$/MAO in CH_2Cl_2/toluene at 20 °C and $P(C_2H_4) = 0.3$ bar: both show very low activity, with that of the carbene adduct (8 kg of PE/((mol of Cr) h)) being 10 times higher than that of the THF adduct.

(34) Margl, P.; Deng, L. Q.; Ziegler, T. *Organometallics* **1998**, *17*, 933.

(35) Jensen, V. R.; Børve, K. J. Manuscript in progress.

(36) Jensen, V. R.; Børve, K. J.; Ystenes, M. *J. Am. Chem. Soc.* **1995**, *117*, 4109.

(37) Margl, P.; Deng, L. Q.; Ziegler, T. *J. Am. Chem. Soc.* **1999**, *121*, 154.

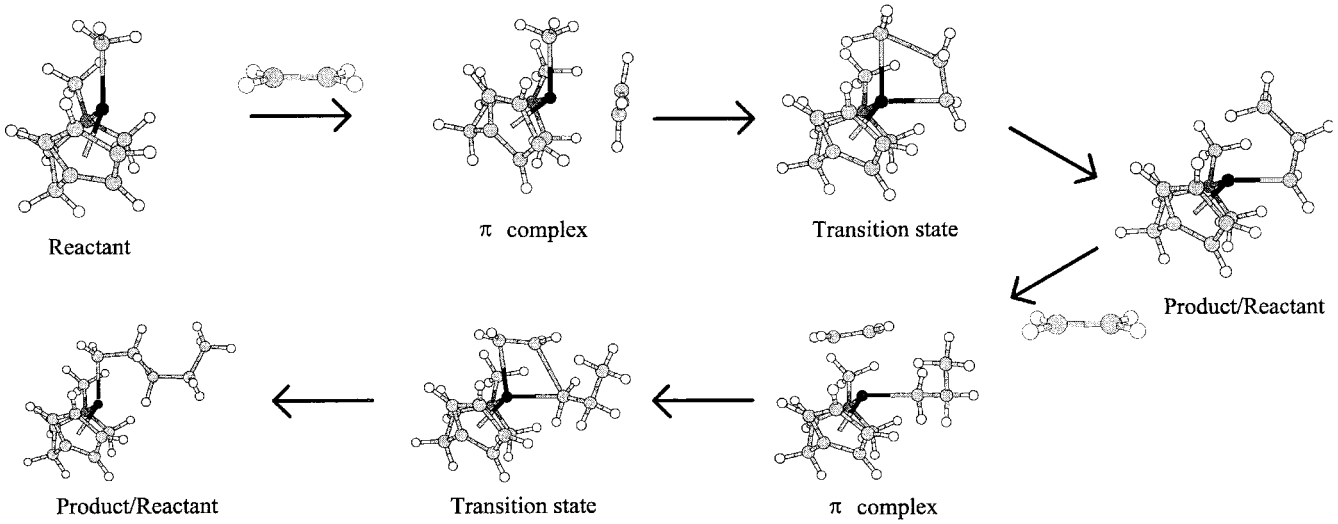

Figure 2. Geometries of stationary points of two consecutive ethylene insertions for $(Me_2NC_2H_4C_5H_4)CrMe^+$ (**5**) as optimized with the ADF approach.

Table 2. Important Structural Parameters of Stationary Points of Ethylene Insertion for Complexes 1−5[a]

complex[b]	Cr−C1	Cr−C3	Cr−Cp[c]	Cr−donor	C1−C2	C2−C3	θ_p[d]
1, R[e]		2.02	1.91	2.06	1.35		0
1, π[e]	2.40	2.07	1.93	2.11	1.37	2.94	28
1, TS[e]	2.10	2.19	1.93	2.12	1.44	2.10	20
2, R[e]		2.03	1.92	2.01	1.35		0
2, π[e]	2.41	2.07	1.95	2.08	1.37	2.91	27
2, TS[e]	2.11	2.19	1.94	2.07	1.43	2.12	19
3, R[e]		2.03	1.93	2.10	1.35		0.5
3, π[e]	2.38	2.07	1.95	2.08	1.38	3.07	30
3, TS[e]	2.10	2.20	1.95	2.09	1.44	2.10	21
4, R[e]		2.00	1.91	2.13	1.35		10
4, π[e]	2.35	2.06	1.94	2.14	1.38	3.10	38
4, TS[e]	2.10	2.18	1.93	2.15	1.44	2.12	29
4, R[f]		2.00	1.92	2.13	1.35		13
4, π[f]	2.37	2.06	1.93	2.14	1.36	3.05	40
4, TS[f]	2.10	2.19	1.93	2.15	1.42	2.10	27
5, R, 1st ins[f]		2.01	1.92	2.15	1.35		9
5, π, 1st ins[f]	2.39	2.06	1.94	2.20	1.36	3.05	37
5, TS, 1st ins[f]	2.11	2.20	1.94	2.20	1.42	2.10	23
5, R, 2nd ins[f]		2.03	1.92	2.17	1.35		18
5, π, 2nd ins[f]	2.45	2.09	1.94	2.22	1.36	3.00	32
5, TS, 2nd ins[f]	2.18	2.15	1.94	2.24	1.39	2.30	23

[a] Bond lengths are given in angstroms and angles in degrees. C1 and C2 denote the two ethylene carbons, with C1 being the atom forming a bond to Cr during insertion. C3 is the alkyl chain carbon next to the metal in the reactant. [b] π symbolizes the chromium−ethylene preinsertion complex and TS the transition state of insertion. [c] The distance between the chromium atom and the geometric midpoint of the five carbon atoms forming the Cp ring. [d] $\theta_p = 360° - \angle$CpCrC $- \angle$CpCr(donor) $- \angle$(donor)CrC, where C denotes the carbon atom closest to Cr in any given structure. [e] G94. [f] ADF.

close to that of a regular tetrahedron. The difference in θ_p of about 10° found between reactant complexes with bridged and free donors is retained in the π complexes as a result of the constrained Cp−Cr−(donor) angle in **4** and **5**. Agostic interactions are not found in the metal−ethylene complexes. The transition states of insertion are located somewhat late, as judged from the forming Cr−C bonds being 8−10 pm shorter than those being broken, as well as relatively long ethylenic bonds of 1.43−1.44 Å. The α-agostic interaction usually found at the transition state (TS) in quantum-chemical studies of metal-catalyzed ethylene insertion is relatively weak for the current complexes, with a lengthening of the C−H bond of only 2 pm. As for d^0 metal-based catalysts,[18] the TS has a more planar character than does the π complex, with a 8−14° lower value of θ_p. The current project is focused on the activation step of going from the π complex to the transition state of insertion. The products of insertion are thus not deemed crucial, and product geometric parameters are not tabulated (except for **5**, for which the product of the initial insertion is tabulated as the reactant of the second). With one exception, the product structures, which have been optimized, show as expected the characteristics of the reactant geometries. The exception is the γ-agostic hydrogen found to be coordinated to the apex of the pyramid formed by the metal and the three primary ligands of the $Cp(donor)CrC_3H_7^+$ complexes, which results in larger values for θ_p.

3.2.2. Energy Profiles. Relative energies for the stationary points of insertion for complexes **1**−**5** are given in Table 3, and the full linear transit energy curve (see Computational Details) describing the shortening of the new C−C bond for the assumed, active component (**5**) of a bridged donor type catalyst is shown in Figure 3. The activation energies range from 6.4 (**2**) to 10.2 kcal/mol (**4**). Part of the variation is a result of the use of two different methods, as is evident when comparing the G94 (8.5 kcal/mol) and ADF (10.2 kcal/mol) values for complex **4**. The higher barrier calculated with ADF is probably due to the fact that in this case true transition states were not identified: the TS is taken as the maximum on the potential energy curve generated by stepwise shortening of the C−C bond formed during insertion. A final transition state optimization starting from this geometry would probably lower the energy to a value closer to the value obtained with G94. Within a single computational approach (G94), the barriers to ethylene insertion vary from 6.4 to 9.2 kcal/mol. If there were no other factors determining catalytic activity, the calculated barrier heights would certainly influence the rate constants; however, the barrier heights show no meaningful correlation with the experimentally recorded activity data. The lowest barrier to ethylene insertion, for example, is found for the THF complex **2**, whereas the complexes relevant to the high-activity catalysts (**4** and **5**) show higher calculated

Table 3. Relative Energies of Ethylene Insertion into the Cr−Methyl Bond in Cp(donor)CrMe$^+$ Complexes 1−5[a]

	energy relative to separated reactants[b]						barrier to insertion[c]	
complex	$\Delta E_e(\pi)$	$\Delta G_{298}(\pi)$	ΔE_e(TS)	ΔG_{298}(TS)	ΔE_e(rx)	ΔG_{298}(rx)	$\Delta E_e^{\ddagger}$	$\Delta G_{298}^{\ddagger}$
1[d]	−16.2	−2.0	−6.9	6.8	−25.6	−9.2	9.2	8.8
2[d]	−11.3	3.1	−4.9	10.7			6.4	7.6
3[d]	−16.5	−3.4	−7.0	7.4	−25.0	−10.4	9.5	10.8
4[d]	−19.8	−6.3	−11.4	4.0			8.5	10.3
4[e]	−19.8		−9.7		−27.3		10.2	
5,[e] 1st ins	−16.3		−6.5		−25.5		9.9	
5,[e] 2nd ins	−8.1		−2.1		−24.3		6.0	

[a] Energies in kcal/mol. [b] π symbolizes the chromium−ethylene preinsertion complex, TS the transition state of insertion, and rx the primary product of the insertion. For **5**, energies are given relative to ethylene + $(Me_2NC_2H_4C_5H_4)CrMe^+$ for the first insertion and ethylene + $(Me_2NC_2H_4C_5H_4)CrC_3H_7^+$ for the second. [c] Energy relative to the π complex. [d] G94. [e] ADF.

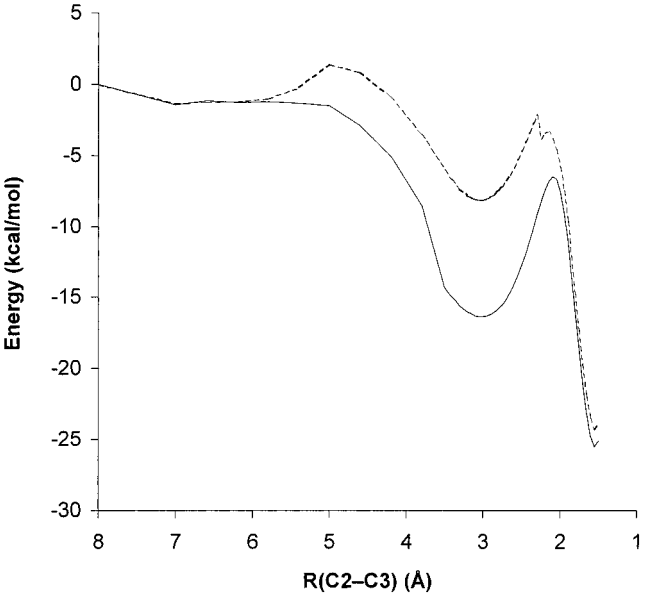

Figure 3. Energy profiles of the first (solid line) and second (dashed line) ethylene insertions for **5** as obtained with the ADF approach. In both cases, energies are given relative to infinitely separated reactants, i.e., relative to ethylene + $(Me_2NC_2H_4C_5H_4)CrMe^+$ for the first insertion and ethylene + $(Me_2NC_2H_4C_5H_4)CrC_3H_7^+$ for the second.

barriers to insertion. Among the higher calculated barriers we also find the carbene complex **3**, whose activity, however, is about 10 times that of the THF complex.[33] In fact, all Cp(donor)Cr^{III}-type complexes tested so far,[9] which either do not contain a donor bridged to the Cp ligand or for which the donor is not coordinated to the metal in the catalyst precursor, are not particularly active. In addition, the calculated barriers are little influenced by the metal−donor bond strength. For example, the two complexes with the weakest (**1**) and strongest (**3**) chromium−donor bond have almost identical barriers to ethylene insertion. In other words, it appears that the dramatic difference in activity among the Cr(III)-based catalysts is not the result of differences in the barrier to insertion.

It could be argued that this lack of correlation between experimental activities and calculated barriers to ethylene insertion is the result of either an oversimplified or perhaps incorrect model for the catalytically active species, that the mechanism followed is incorrect, or that the calculations themselves are simply not sufficiently accurate. In contrast to the group 4 metallocene catalysts, for which the active center has been identified[38] and for which a series[17,18,34,36,37] of theoretical investigations support the Cossée−Arlman mechanism, the nature of the active species in the case of chromium has not been identified. However, there is convincing evidence that the active center and mechanism postulated here are reasonable. Investigations of systems such as $[CrCp^*(THF)_2Me]^+BPh_4^-$ indicate that the active component of this catalyst is actually the mono-THF 13-electron chromium(III) cation.[5] Attempts to design related chromium(II)-based catalysts have not been successful,[5] while excess THF reduces the polymerization activity of the Cr(III)-based catalyst. Furthermore, a 15-electron species such as the $[CrCp^*(THF)_2Me]^+$ cation may be regarded as a coordinatively saturated, relatively stable entity,[6,39] as can the corresponding mono-THF ethylene complex. Our calculations also indicate that, with ethylene present, the resulting 15-electron species are both electronically and coordinatively saturated. In attempts to explore two-monomer mechanisms, it became apparent that such 17-electron species are unstable, and the second ethylene molecule is invariably expelled from the coordination sphere of chromium during the geometry optimizations. In addition, the similarity with the group 4 based catalysts is also evident from our results as well as from the earlier[13] quantum-chemical investigation: the insertion process proceeds through almost identical stationary points, although with a somewhat higher barrier to insertion than found for the group 4 metallocenes (see below for comparison). However, the energy profiles reflect that insertion for Cr(III)-based 13-electron reactants is a highly feasible reaction, and it is not easy to envisage a mechanism that could proceed with a lower barrier.

We have previously shown[22] that, as far as modeling of ethylene insertion is concerned, the DFT functional applied in the present work (BPW91) performs in excellent agreement with the best ab initio methods available. The only available experimental estimate (8 kcal/mol[11]) of an activation energy for a homogeneous, chromium(III)-based catalyst falls in the middle of our calculated values. In fact, even $Cl(H_2O)CrMe^+$, a minimal model of a Cr(III)-based catalyst, was found to display a barrier to ethylene insertion close to 8 kcal/mol,[13] confirming that the barrier to ethylene insertion is determined to a large extent by the electron configuration of the metal (d^3, molecular term symbol ^4A) rather than by the exact nature of the ligands. There is hence sufficient reason to expect that differences in

(38) Jordan, R. F.; Dasher, W. E.; Echols, S. F. *J. Am. Chem. Soc.* **1986**, *108*, 1718.
(39) Green, M. L. H. *J. Organomet. Chem.* **1988**, *500*, 127.

activation energy calculated within a series such as the current one should be reproduced accurately.

Having established that the calculated electronic barriers for the Cr(III) species fall in the range 6−10 kcal/mol, it is of interest to compare these d^3 systems with the group 4 catalysts which have no formal d occupation. Woo et al.[40] have reported barriers to insertion into the zirconium−methyl bond of Cp_2ZrMe^+ and $SiH_2(Cp_2)ZrMe^+$ to be below 1 kcal/mol using gradient-corrected DFT methods comparable to the those discussed here, and a somewhat higher barrier[13] was also noted for the simple model system $Cl(H_2O)$-$CrMe^+$ in comparison to corresponding chlorides of group 4. The origin of these differences is probably electronic and can be assigned to a difference in the ability of d^0 and high-spin d^3 metal atoms to take part in the insertion reaction. One significant difference between d^0 metals and metals with formal d occupation is the tendency of the latter to form covalent bonds with alkenes through donation of metal d electrons into the π^* orbital of the alkene. At the TS of insertion, contribution from π^* is important for forming the new C−C bond and, in the case of a d^0 metal, the accompanying $\pi-\pi^*$ mixing leaves the complex with a relatively high-lying LUMO of antibonding ethylene−alkyl character.[18,41] Population of this antibonding orbital at the TS through substitution of the d^0 metal with, for example, a d^3 metal should therefore lead to a higher activation energy. In our chromium(III) π complexes, the back-donation bond to ethylene is, as expected, found among one of the three singly occupied orbitals (SOMO's). At the TS of insertion, however, the energy of the π^*-rich antibonding ethylene−methyl orbital is too high to be retained among the SOMO's, which are seen to be dominated by metal d orbitals. The higher activation energy calculated for the d^3 metal based catalysts may thus be explained as originating at the cost of breaking the back-donation metal−ethylene bond in the pre-insertion complex rather than as being due to the involvement of an ethylene−alkyl antibonding interaction at the TS. Similar findings have been made for related first-row transition-metal systems having the oxidation state +III.[42] Finally, from the treatment of the monomer-free reactants (see above), it should be recalled that the three-coordinate Cr(III)-methyl complexes have no or insignificant barriers toward planarity. This property is of importance for maintaining a low barrier to insertion,[18,35] and in this respect the Cr(III) complexes have an advantage over many of the d^0 systems. To summarize, the title d^3 chromium(III)-based catalysts have electronic properties which both facilitate and hinder insertion compared to typical d^0 metal catalysts. The height of the activation barriers, however, suggests that the latter do have a slightly higher intrinsic ability to perform insertion.

Total reaction energies are not crucial to the present project, and only a few have been calculated. The absolute values are in the range 25−27 kcal/mol and reflect the overall reaction energy for the simple gas-phase reaction $CH_3 + C_2H_4 \rightarrow C_3H_7$ (−27.6 kcal/mol with the G94 approach). The ethylene coordination energies are of more relevance to the barrier heights, although at first glance no simple correlation is apparent. However, it is probably no coincidence that the complex **2**, with the lowest ethylene coordination energy, has the lowest barrier to insertion. The steric bulk of the THF complex is apparently sufficiently large to lower the stability of the π complex, relative for example to that of the water complex (**1**), and thus to reduce the energy needed to perform insertion from the latter. It should also be noted that the calculated ethylene coordination energies are low compared to those obtained for the donors in Table 1. Displacement of the donor through monomer coordination thus proceeds only in the presence of excess alkene. However, in the vicinity of complexes such as **4** and **5**, the donor concentration will always be large and increasing the concentration of alkene should not be expected to have the same effect on displacement. For the amino-substituted Cp−chromium catalysts, a propagation mechanism involving displacement of the donor group through monomer coordination is not a necessity.

Mainly because of the reduction in entropy upon coordination, the Gibbs free energies, as compared to electronic energies, are much less in favor of the π complexes. For the present catalysts, the $-T\Delta S$ contribution is 10.6−12.6 kcal/mol at 25 °C and increases by another 1.3−1.4 kcal/mol at 60 °C. In general, the free energy of formation of π complexes from infinitely separated catalyst and ethylene entities is seen to be close to zero for the approach of the first ethylene molecule. In fact, for **2**, the free energy of coordination is already positive at ambient temperatures. As the electronic stabilization will be lower for coordination of the second ethylene molecule (see below) and also for catalysts including ligands with bulky substituents,[43] free energies of coordination should generally be expected to be even less in favor of the π complex than those calculated here. The presence of solvent molecules and counterions (cocatalyst) will also contribute to a less favorable coordination of the monomer. It is possible that, at least for some of the homogeneous Cr(III)-based catalysts described here, the coordination step is actually rate-determining. Unfortunately, an accurate estimate of the free energy of π coordination, or the height of the barrier involved in this step, including all the factors mentioned above, is not feasible at the current stage. In principle, the large difference in catalytic activity observed between THF complexes and the bridged amino complexes could be caused by differences in coordinating the monomer, as indicated by our calculated coordination energies. However, experimental evidence[9] suggests that steric hindrance during ethylene coordination actually is not the only reason for this difference: one of the major structural differences between the C_2H_4-bridged and the free-donor complexes is the more acute Cp−Cr−(donor) angles of the former resulting from a short bridge, leaving a larger metal surface available for ethylene coordination. However, increasing the length of the bridge from C_2H_4 to C_3H_6 has been observed to have no influence on the catalytic activity. Also, one of the most active catalysts so far tested is the rather bulky compound (cyclo-$C_4H_8NC_2H_4C_5$-

(40) Woo, T. K.; Fan, L.; Ziegler, T. *Organometallics* **1994**, *13*, 2252.
(41) Lauher, J. W.; Hoffmann, R. *J. Am. Chem. Soc.* **1976**, *98*, 1729.
(42) Jensen, V. R.; Angermund, K.; Jolly, P. W. Manuscript in progress.
(43) Thorshaug, K.; Støvneng, J. A.; Rytter, E.; Ystenes, M. *Macromolecules* **1998**, *31*, 7149.

Me_4)$CrMe_2$, where the donor group is structurally similar to tetrahydrofuran.

3.3. Second Ethylene Insertion. As noted already for the products of the first insertion step, the chromium−propyl cations display marked γ-agostic interactions, with a lengthening of the C−H bond of 3 pm. This secondary interaction reduces the acidity of the reactant complex for the second and later insertion steps compared to that of the methyl fragment. Accordingly, the exothermicity of the ethylene coordination step is significantly lowered, as is evident from the potential energy curve shown in Figure 3 as well as the relative energies given in Table 2. The electronic barrier for displacement of the γ-agostic hydrogen is estimated to be around 3 kcal/mol, from the weak charge-induced-dipole complex seen at large C2−C3 distances. Insertion from the π complex proceeds rapidly, with a barrier of ca. 6 kcal/mol—some 4 kcal/mol lower than that of the first insertion. This is mainly a result of the slightly reduced stability of the π complex. As judged from the fact that the new chromium−carbon bond is longer than the one to be broken, the TS is located earlier (see Table 2 and Figure 2) than all of those found for the initial insertion, where bond-breaking and -forming seemed to be the dominating process in the transition-state region. No vibrational analysis was performed for the maximum on the linear transit curve seen in Figure 3, but a comparison of the structures of neighboring points around the TS confirms that internal rotations of the alkyl chain are also important at this stage of the reaction. As expected, due to reduced acidity of the the Cr−propyl compared to the Cr−methyl cation, the overall exothermicity of the second insertion is somewhat lower than that of the first. The energy curve of the second insertion is less pronounced and is similar to those obtained for second and later insertion for γ-agostic structures of zirconocene-based catalysts.[43] It can be expected that structures and reaction profiles of other reaction routes, not covered in the present study, will be similar to those obtained in the detailed studies of zirconocene-based catalysts.[43]

As we have already mentioned for the first insertion step, the reduction in entropy upon coordination could result in an increase in the corresponding free energy of activation during formation of the π complex compared to the $\Delta G^{\ddagger}$ of insertion, and further studies directed toward the coordination step will be needed to clarify this point. Despite the electronic configuration on the d^3 metal being somewhat less suited to alkene insertion than that of d^0 metals, it appears that these differences become less significant for the actual catalytic complexes and subsequent insertions. In the π complex region, bulky substituents and the presence of longer polymer chains result in a more loosely bound monomer with a π^* population lower than that found in the smaller Cr−methyl complexes. With the barrier reduced to ca. 6 kcal/mol, the insertion step is indeed facile and does not represent a serious bottleneck in the propagation cycle. Our computational results are thus consistent with the experimental finding that the bridged, amino-substituted CpCr/MAO catalysts[9] are very effective polymerization catalysts, with activities comparable to those of the group 4 based metallocene/MAO systems.

4. Conclusions

The Cp(donor)$CrMe^+$ complexes (**1**−**5**) were found to insert ethylene with activation barriers in the range 6−10 kcal/mol. These barriers are, as expected, somewhat higher than those found for comparable group 4 metallocene species. The higher barrier is mainly associated with the breaking of the back-donation bond upon going from the preinsertion ethylene complex toward the transition state of insertion. However, for realistic catalytic complexes and subsequent insertions, it is seen that some compensation of the d^0/d^3 difference occurs. The calculations also show that the insertion step for the Cr(III)-based catalysts does not represent a serious bottleneck in the propagation cycle, and this is consistent with the high activities of the amino-substituted Cp−Cr catalysts.

The trend among the calculated barriers to ethylene insertion for the Cp(donor)$CrMe^+$ complexes does not, however, correlate with the corresponding metal−donor bond strengths or the experimental observation that catalysts with donor-substituted Cp ligands are more active than those with free, unbridged donor groups. The difference in activity is, therefore, not the result of a different ability of the various Cp(donor)CrR^+ complexes in performing the bond-breaking and -forming phases of the Cossée−Arlman-type insertion step. An alternative explanation for the differences in activity focuses on the role of the bridge in the donor-substituted Cp−Cr catalysts: the calculated Cr−donor bond strengths for the Cp(donor)$CrMe^+$ species are considerably larger than the corresponding Cr−ethylene and Me_3Al−donor bond strengths. For catalysts with free donors used in combination with MAO or a classic cocatalyst such as $AlMe_3$, the donor will probably dissociate from the chromium complex as a result of the high Al:Cr ratio and the presence of solvent. A bridge linking the donor group and the cyclopentadienyl fragment, however, ensures a high donor concentration in the vicinity of the metal, regardless of the bulk concentrations of cocatalyst and monomer. This suggests that the presence of the donor in the inner coordination sphere of the metal is essential for high activity. At the present stage, we have no evidence supporting the existence of a more dynamic behavior[44] of the bridged donor group.

Acknowledgment. This research was financially supported by The Norwegian Academy of Science and Letters together with Statoil (VISTA, Grant No. V6415) as well as the Research Council of Norway (Grant No. 119204/410). Access to supercomputer resources was granted by the Research Council of Norway (Program for Supercomputing), the Rechenzentrum der Gesellschaft für wissenschaftliche Datenverarbeitung in Göttingen, Germany, and the Rechenzentrum der MPG und IPP in Garching, Germany.

OM9906666

(44) Jutzi, P.; Redeker, T. *Eur. J. Inorg. Chem.* **1998**, 663.
(45) Schaftenaar, G. Molden 3.5; University of Nijmegen, Nijmegen, The Netherlands, 1999.